Cement and Concrete Research 49 (2013) 48–54

Contents lists available at SciVerse ScienceDirect

Cement and Concrete Research

journal homepage: http://ees.elsevier.com/CEMCON/default.asp

New data on the thermal behavior of 14 Å tobermorite

Cristian Biagioni [a], Elena Bonaccorsi [a,*], Stefano Merlino [a], Danilo Bersani [b]

[a] Dipartimento di Scienze della Terra, Università di Pisa, Via Santa Maria 53, I-56126 Pisa, Italy
[b] Dipartimento di Fisica, Università di Parma, Viale G.P. Usberti 7/a, I-43100 Parma, Italy

ARTICLE INFO

Article history:
Received 13 July 2012
Accepted 13 March 2013

Keywords:
Thermal treatment (A)
Calcium–silicate–hydrate (C–S–H) (B)
Crystal structure (B)
X-ray diffraction (B)
Spectroscopy (B)

ABSTRACT

The thermal behavior of two specimens of 14 Å tobermorite (plombièrite) was studied in situ at the GILDA beamline (ESRF, Grenoble, France). During dehydration, plombièrite shortens its basal spacing from 14 to 11 Å, through a progressive approaching of the complex structural modules characterizing its crystal structure. Upon heating, the 11 Å phase progressively contracts its *c* periodicity, with its d_{002} varying from 11.7 to 11.3 Å. At ca. 300 °C, a 9.6 Å phase appears; it is stable up to ca. 700 °C. Above this temperature, it expands its basal spacing up to 10.2 Å, before transforming into wollastonite.
Moreover, one specimen was heated at 150 °C for 4 h and the heated product, identified as 11 Å tobermorite through X-ray powder diffraction, was used to collect micro-Raman spectra. The heated product shows single chains, in contrast with the 11 Å natural specimens studied up to now in which double wollastonite-like chains occur.

1. Introduction

Plombièrite belongs to the tobermorite group, a series of calcium silicate hydrates (C–S–H) studied for their relationship with the main binding agent of the Portland cement and for their potential technological applications. These phases may be distinguished on the basis of their basal spacings, that are related to their different degrees of hydration. In particular, plombièrite, with a basal spacing of 14 Å, is the most hydrated member of this group.

The name plombièrite was firstly used in [1] for a C–S–H gel formed through the action of thermal springs on Roman cementitious material at Plombières, Vosges, France; probably, the original material belongs to the C–S–H (I) group [2]. On the basis of the chemical similarity between this nearly amorphous material and a crystalline compound from Ballycraigy, the use of the name plombièrite was extended in [3] to the 14 Å phase of the tobermorite group. Therefore, this name has been traditionally retained in the mineralogical community. In the following we will use the name plombièrite to indicate the natural phase, whereas the synthetic counterpart will be called 14 Å tobermorite.

The ideal chemical formula of plombièrite is $Ca_5Si_6O_{16}(OH)_2 \cdot 7H_2O$. Its crystal structure has been solved [4] using a specimen from Crestmore (California, USA). The atomic coordinates of one of the two possible MDO polytypes were derived on the basis of the OD theory and were refined using intensity data collected both with laboratory and synchrotron X-ray sources [4]. The crystal structure of plombièrite (Fig. 1) is formed by the same complex structural module characteristic of 11 Å tobermorite. In the crystal structure of plombièrite, complex structural modules with chemical composition $[Ca_4Si_6O_{16}(OH)_2 \cdot 2H_2O]^{2-}$ are shifted each other of **b**/2 along [010] and are separated by an interlayer of H_2O molecules and Ca^{2+} cations. Consequently, the wollastonite-like silicate chains are not connected and remain single (*Dreiereinfachketten*; [4,5]).

The thermal behavior of plombièrite – as reported in literature – is apparently simple: at 80 °C–110 °C, its *c* parameter shrinks to 11 Å; at 300 °C, the latter reduces to 9 Å. Above 800 °C–1000 °C the 9 Å phase recrystallizes into wollastonite. This is actually an oversimplification of a more complex behavior. The appearance of a 10 Å phase was observed [6] by heating specimens of plombièrite from Crestmore and Bingham above 700 °C. Plombièrite from Crestmore was studied also in [7] and the presence of an intermediate phase between tobermorite 9 Å and wollastonite, with a basal spacing of 9.7 Å was detected at 770 °C. In [6] a 10.1 Å basal spacing was reported at 900 °C.

Another intriguing aspect is related to the real nature of the 11 Å phase formed through the dehydration of plombièrite. According to [8] and [9], the so-called molybdate method and ^{29}Si NMR data, respectively, suggested that this 11 Å phase has single *dreierketten*, whereas all known natural and directly synthesized 11 Å tobermorites have double wollastonite-like chains. The thermal behavior of synthetic 14 Å tobermorite was studied also by [10]; the authors described the dehydration process of a hydrothermally synthesized sample outlining the formation of a 11.8 Å tobermorite that shrinks to 11.3 Å tobermorite at 250 °C, before the final shrinking into a 9.6 Å phase. ^{29}Si NMR spectra collected on dehydration products of 14 Å tobermorite, obtained at different temperatures, showed the presence of single chains in the 11.8 Å tobermorite, and the possible occurrence of Q^3 sites in 11.3 Å tobermorite and, maybe, in the 9.6 Å phase [10].

* Corresponding author.
E-mail address: elena@dst.unipi.it (E. Bonaccorsi).

0008-8846/$ – see front matter © 2013 Elsevier Ltd. All rights reserved.
http://dx.doi.org/10.1016/j.cemconres.2013.03.007

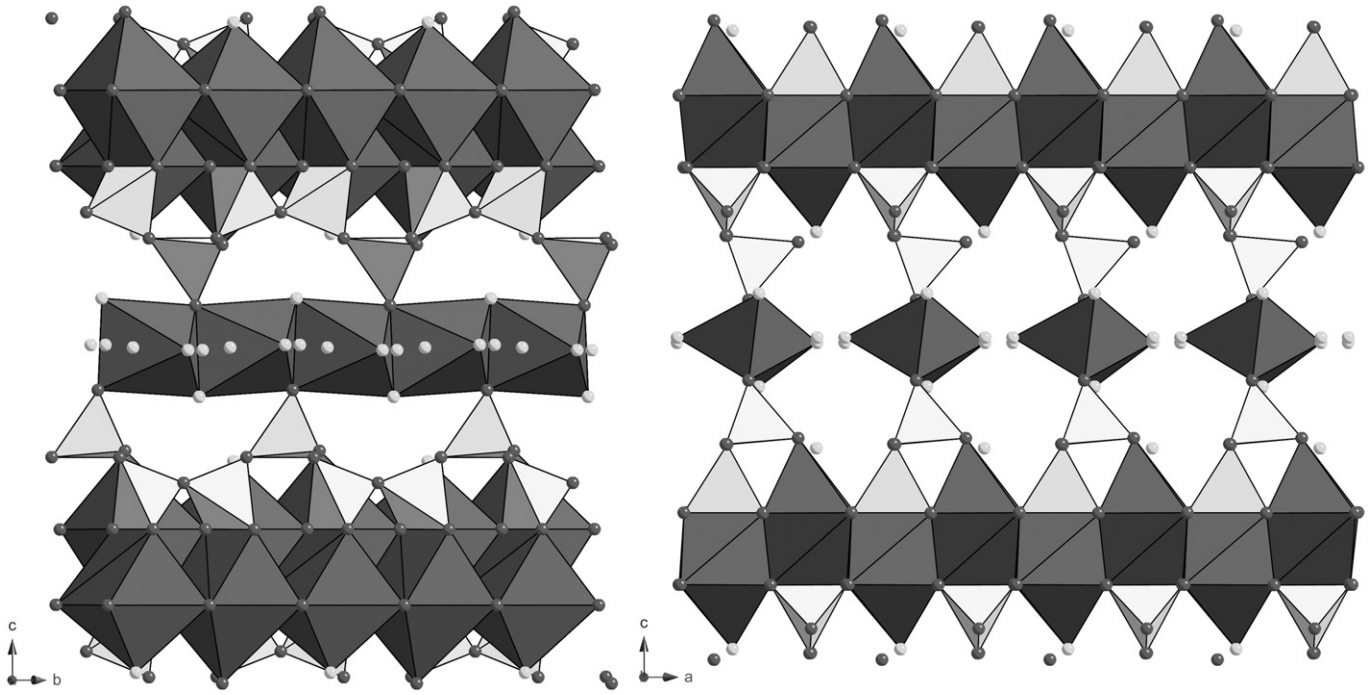

Fig. 1. Crystal structure of plombièrite, as seen down [100] on left and [010] on right. The calcium-centered polyhedra are drawn in dark gray whereas the SiO_4 tetrahedra are shown in light gray. Oxygen atoms and hydroxil groups are indicated as dark gray circles and H_2O molecules are represented as light gray circles. Along [010] the apical sites of the seven-fold coordinated Ca-centered polyhedra are alternatively occupied by $(OH)^-$ groups whenever they are shared with an SiO_4 tetrahedron, and by H_2O molecules if not shared.

Natural specimens of plombièrite from Fuka (Okayama Prefecture, Japan), intimately associated with tobermorite, were studied and described in [11]. During the first part of the heating process, a 11 Å phase characterized by single chains formed, whereas 9 Å tobermorite appeared above 300 °C. According to these authors, the broadness of the 002 reflections of both 11 and 9 Å phases suggested the possible existence of a phase with an intermediate spacing.

The aim of this paper is the description of the thermal behavior of two specimens of plombièrite from Crestmore (California, USA), and one specimen from the Zeilberg quarry (Bavaria, Germany). The samples were studied through X-ray diffraction and their behavior has been compared with those described in the previous works on natural and synthetic 14 Å tobermorites. Finally, one of the two samples from Crestmore was used for the collection of micro-Raman spectra on both unheated and thermal-treated samples.

2. Materials and methods

Plombièrite from Crestmore (California, USA) and the Zeilberg quarry (Bavaria, Germany) were investigated. Two specimens from Crestmore were used: in the former few micrometric single crystals were selected for micro-Raman spectroscopy, before and after heating; they were picked up from the same sample used for the determination of the crystal structure [4]. The second sample from Crestmore was a white crust of microcrystalline 14 Å tobermorite kindly given to us by the late Prof. H.F.W. Taylor; it was crushed and used for the in-situ thermal study.

In situ time-resolved X-ray powder diffraction (TR-XRD) patterns were collected in the Debye Scherrer transmission geometry, with samples contained in a 0.5 mm amorphous silica capillary at the GILDA (General Italian Line for Diffraction and Absorption) of the ESRF (Grenoble, France) synchrotron facility, using the same experimental apparatus described in [12]. The two slits in front of the image plate (IP) allowed the selection of a vertical slice of the Debye rings generated by the diffracting powder, which rotated about the φ axis while the recording IP support linearly translated, with constant speed, behind the slits. Consequently, the diffraction pattern was recorded as a function of time and sample treatment. This experimental setup allowed us to collect a continuous diffraction pattern while the sample was heated by a hot air blower.

Sample to detector distance and detector tilt were carefully calibrated against standard LaB_6 (SRM 660a). The calibration of the heating apparatus was performed by measuring accurate Rietveld refined lattice parameters of standards with known thermal expansion coefficient [12]. The data stored in the latent image were recovered and digitized using a Fuji BAS-2500 laser scanner with a $100 \times 100\ \mu m^2$ pixel size and a dynamic range of 16 bit/pixel. The digitized images were integrated using the FIT2D [13] software to have intensity vs 2θ diffraction patterns.

The sample from Crestmore was heated from room temperature (25 °C) up to 960 °C, with a heating rate of ca. 2.4 °C/min. Initially, the powder sample was maintained at 25 °C for 15 min, then heated up to 960 °C. Finally, it was maintained at the final temperature for 15 min. The radiation wavelength was set at $\lambda = 0.687337$ Å; the measured 2θ ranges between 2° and 40°.

The sample from Zeilberg was heated from room temperature (30 °C) up to 950 °C, with a heating rate of ca. 7.7 °C/min. The radiation wavelength was $\lambda = 0.783485$ Å; the measured 2θ range is 2.5°– 40°.

The cell parameters were refined using the GSAS program [14] with the EXPGUI graphical user interface [15]. The refinements of the cell parameters were carried out by means of the Le Bail method [16]. The background was fitted with a shifted-Chebyshev function, using 18 terms for the specimen from Crestmore and a number of terms ranging from 12 to 24 for the German plombièrite; the profile shape was modeled by Pseudo-Voigt functions, refining the Gaussian parameter GW, the Lorentzian parameters LX and LY, and the asymmetry of the peak profiles.

Crystals of plombièrite from Crestmore were heated at 150 °C for 4 h and used for the collection of X-ray powder diffraction patterns using a 114.6 mm Gandolfi camera with Ni-filtered Cu *K*α radiation. These crystals were used for the collection of micro-Raman spectra in nearly backscattered geometry with a Jobin-Yvon Horiba “Labram”

apparatus with a 1800 lines/mm grating and equipped with a motorized *x*–*y* stage and an Olympus BX40 microscope with a 50× objective (NA 0.75). The 632.8 nm line of a He–Ne laser (15 mW) was used; laser power was controlled by means of a series of density filters. The reported measurements were obtained using a ND1 filter. The power on the sample is then 1.5 mW, resulting in an estimated radiation power of 50 kW/cm^2. The input slit was set to 150 μm, resulting in a minimum lateral resolution of 3 μm and an estimated depth resolution of 6 μm. The system was calibrated using the 520.6 cm^{-1} Raman band of silicon before each experimental session. The spectral resolution is 2 cm^{-1} while the spectra accuracy, estimated by Gauss–Lorentzian interpolations after calibration, is 0.5 cm^{-1}. Spectra were collected with multiple acquisitions (2 to 6) with single counting times ranging between 20 and 180 s. Micro-Raman spectra were collected for both the unheated plombièrite and the heated product. Peaks were fitted through the software FITYK [17].

3. X-ray diffraction results

The results of the X-ray diffraction studies performed on the specimens from Crestmore and Zeilberg will be described separately.

3.1. Plombièrite from Crestmore (California, USA)

Plombièrite from Crestmore was used both for in situ and ex situ thermal studies. The ex situ study was performed in order to obtain suitable material for micro-Raman spectroscopy, aiming to the study of the degree of polymerization of silicate tetrahedra.

3.1.1. In situ study

The X-ray powder diffraction pattern collected at room temperature showed that the sample was polyphasic; in addition to the most abundant phase plombièrite, the presence of oyelite and minor 11 Å tobermorite was detected. The association of plombièrite and oyelite in the deposit of Crestmore is well-known and the amount of B_2O_3 reported in some analyses of plombièrite from this locality, e.g. in [6], could be due to the admixture of oyelite.

The sub-cell parameters of plombièrite and tobermorite were used as starting values for the unit-cell parameter refinements; the crystallographic parameters of oyelite are those of the sub-cell measured on a crystal from the N'Chwaning II mine (Kalahari Manganese Field, Republic of South Africa) with an Oxford Xcalibur S four-circle diffractometer and CCD detector [18], i.e. *a* 3.6131(6), *b* 5.557(1), *c* 20.457(2) Å, α 90.77(2), β 90.38(2), γ 90.27(2)°. The refinement was conducted up to the disappearance of the 11 Å phase, at ca. 300 °C; at this temperature, a broad and weak 9.6 Å basal reflection appeared. Fig. 2 shows the X-ray powder patterns. In the temperature range 100 –118 °C the basal reflection of plombièrite progressively shifts towards higher 2θ angles and weakens, completely disappearing at ca. 118 °C; Fig. 3a shows the variation of the parameters of this phase as a function of temperature, normalized to the value at room temperature. Whereas the *a* and *b* cell parameters do not change significantly, the **c** axis shortens above 100 °C. The constancy of the values of the **a** and **b** axes suggest that the complex structural modules described in the "Introduction" section do not change and that the dehydration causes only their approaching.

The same trend was also observed for the newly formed 11 Å phase that appears at 110 °C, coexisting for ca. 10 °C with plombièrite. It is important to stress the difference in the basal spacings between the two 11 Å phases observed during the thermal study of the specimen from Crestmore; in fact, whereas the 11 Å tobermorite coexisting with plombièrite and oyelite at room temperature has a basal spacing of ca. 11.25 Å, the 11 Å phase formed through the dehydration of plombièrite has a longer **c** axis, with a d_{002} of 11.7 Å.

Above ca. 118 °C, plombièrite completely disappears. A progressive shortening of the **c** axis of the newly formed 11 Å phase can be observed (Fig. 4a), in agreement with the study of [10], from 23.4 Å down to 22.45 Å, corresponding to a shift in the basal spacing d_{002} from 11.7 to 11.22 Å.

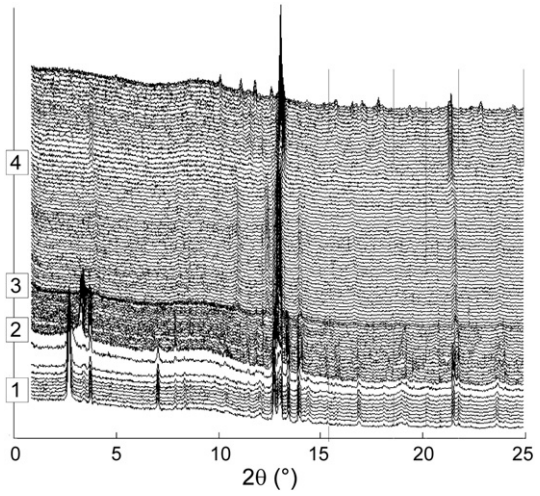

Fig. 2. X-ray powder diffraction patterns of plombièrite from Crestmore, from room temperature up to 960 °C. (1) At T = 25 °C the sample contains mainly plombièrite and oyelite; (2) at ca. 118 °C plombièrite disappears being substituted by 11 Å tobermorite; (3) at ca. 300 °C 11 Å tobermorite is replaced by 9 Å tobermorite, while oyelite disappears; (4) above 700 °C the very weak basal reflection of 9 Å tobermorite shifts towards lower angle values.

At ca. 286 °C, both 11 Å tobermorite and oyelite disappear, with the appearance of a 9.6 Å phase. The basal reflection of this newly formed phase is weak and broad, indicating a high structural disorder along **c**; the other classes of reflections remain intense and relatively narrow.

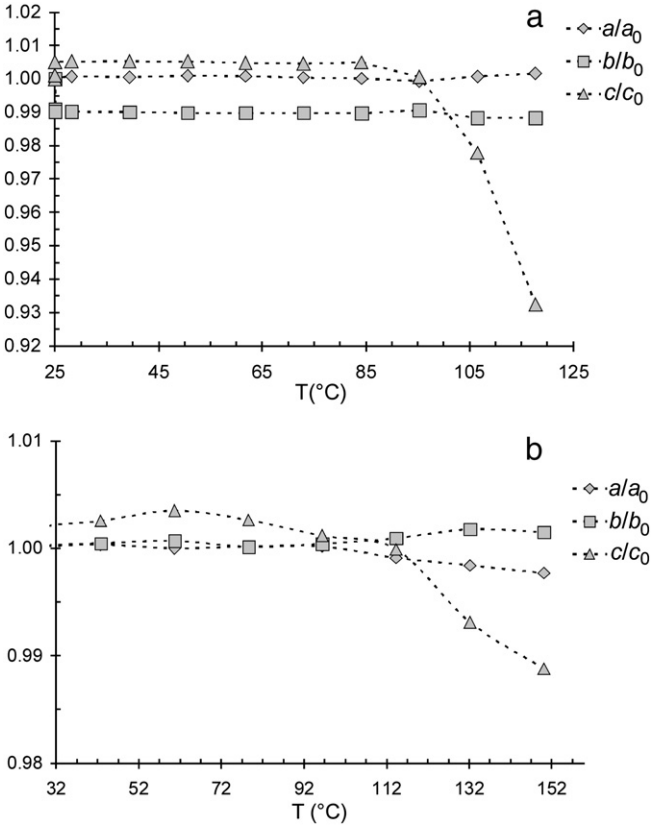

Fig. 3. Trend of the ratio between the refined cell parameters and the parameters at room temperature for the sample from Crestmore (a) and Zeilberg (b).

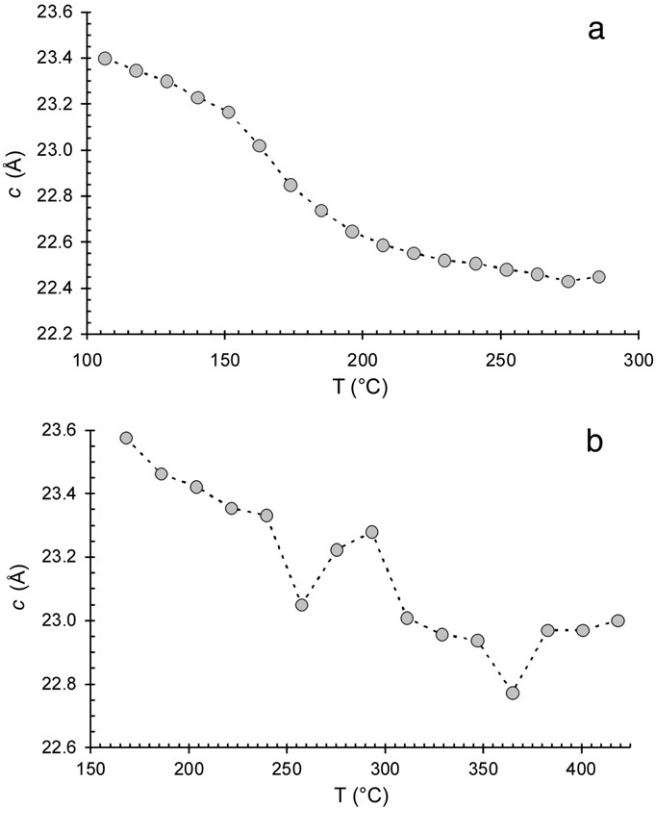

Fig. 4. Variation of the *c* parameter (in Å) for the 11 Å tobermorite formed by the dehydration of plombièrite from Crestmore (a) and Zeilberg (b).

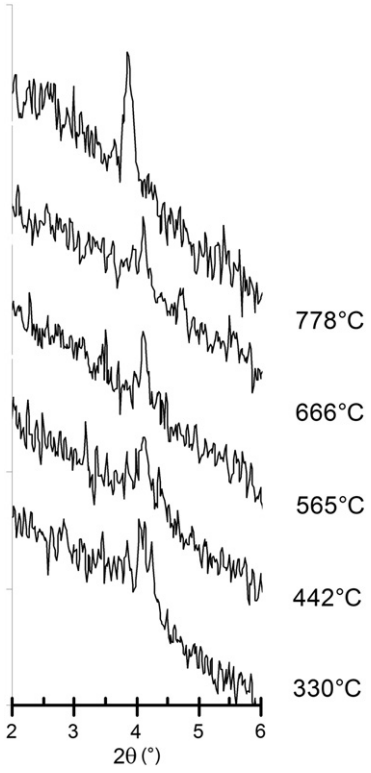

Fig. 5. Behavior of the basal spacing of the 9.6 Å tobermorite as a function of temperature.

Increasing the temperature, the basal reflection shifts towards lower 2θ values (Fig. 5), up to the appearance, at ca. 720 °C, of a phase with a basal spacing of 10.2 Å, preceding the crystallization of wollastonite, at ca. 880 °C.

3.1.2. Ex situ study

An interesting topic related to the thermal behavior of plombièrite is the nature of the silicate chains in the 11 Å phase produced by the dehydration of the 14 Å one. According to some experimental works [8–10], the dehydration of synthetic 14 Å tobermorite produces 11 Å tobermorite with single wollastonite-like chains, with only a minor amount of double wollastonite-like chains above 250 °C.

Owing to the low amount of available material, the polymerization of the silicate chains was studied through micro-Raman spectroscopy on small single crystals. For this reason, some crystals of plombièrite, previously identified through X-ray powder diffraction, were heated at 150 °C for 4 h. The heating product was identified as 11 Å tobermorite through the same technique. Fig. 6 shows the powder patterns of plombièrite before and after the thermal treatment. A general broadening of the diffraction effects can be observed, resulting from increasing disorder in the stacking of complex layers. The diffraction pattern of the dehydrated product is similar to that of natural 11 Å tobermorite.

3.2. Plombièrite from Zeilberg (Bavaria, Germany)

The X-ray diffraction pattern collected at room temperature showed that also the powder sample of the specimen from Zeilberg was polyphasic; in addition to plombièrite, that was the most abundant phases, 11.7 Å tobermorite as well as ettringite are present. Ettringite, ideally $Ca_6Al_2(SO_4)_3(OH)_{12}\cdot 26H_2O$, crystallizes in the space group $P6_3/mmc$, with cell parameters *a* 11.23 and *c* 21.48 Å [19].

During the study of the thermal behavior of plombièrite from Zeilberg, the same transition observed in the sample from Crestmore was observed, even if at a higher temperature. This may be caused by the faster heating rate used during the in situ study of the German plombièrite. In fact, plombièrite disappeared at ca. 150 °C, whereas the 9 Å phase crystallized at 360 °C. Ettringite disappeared below 130 °C, in agreement with several studies on the thermal behavior of this mineral [19–24].

Fig. 3b shows the trend of the cell parameters of plombièrite from Zeilberg, as a function of temperature, normalized to the cell constants at room temperature. 11 Å tobermorite is present in the studied sample at the beginning, with a d_{002} of 11.65 Å. Such a high value is usually related to high Al content in natural tobermorites [25]. For the studied specimen from Zeilberg, chemical data are missing; however, due to the association with ettringite, it is possible that Al may partially replace

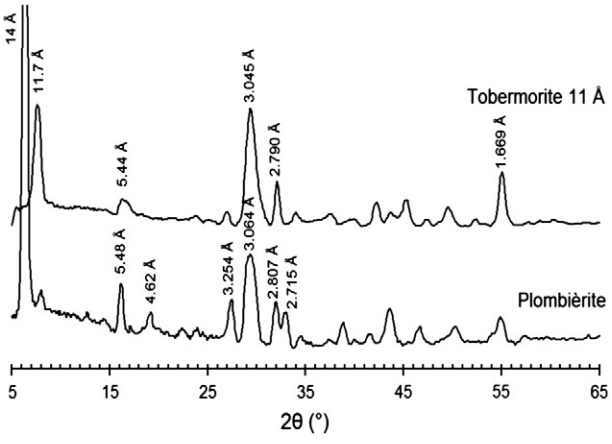

Fig. 6. X-ray powder diffraction patterns of plombièrite from Crestmore and its heating product at 150 °C for 4 h. For sake of clarity, the values d_{hkl} of the most intense reflections are shown.

Si in the bridging tetrahedra of tobermorite. Beginning from 150 °C, the intensity of the 002 reflection of tobermorite 11 Å increases, whereas that of plombièrite abruptly decreases. The angular position of the reflection of the 11 Å phase shifts towards lower 2θ values, achieving a basal spacing of ca. 11.8 Å. At ca. 168 °C, plombièrite is no longer present in the studied sample. Fig. 4b shows the variation of the *c* parameter of the 11 Å phase from this temperature up to its complete transformation into the 9 Å phase. As observed for the specimen from Crestmore, also in this sample a decrease in the basal spacing of the newly formed 11 Å tobermorite is observed. The irregularity in the decreasing trend can be an artifact due to the worse quality of the data, collected with a higher heating rate than that used for the specimen from Crestmore.

The 9 Å phase appears above 360 °C; at 430 °C it is the only phase in the powder sample. The intensity of its basal reflection, at 9.6 Å, is very weak and the peak is very broad. On the contrary, the other classes of reflections remain relatively intense and narrow, probably indicating that the high degree of disorder is mainly related to the stacking along the direction normal to (001).

4. Micro-Raman spectroscopy results

Micro-Raman spectra were collected both on plombièrite and on the dehydrated 11 Å phase. Fig. 7 and Table 1 report the spectra and the observed frequencies, respectively. The main bands are related to stretching and bending vibrations of Si–O bonds (Fig. 8). The most intense band in the spectrum of plombièrite is at 664 cm^{-1}, and it is due to bending vibrations of Q^2 tetrahedra; an additional weaker band is present at 680 cm^{-1}, contributing to the asymmetry towards higher frequencies of the main band. In the region of the stretching vibrations of Si–O bonds, three bands occur, i.e. at 996 cm^{-1}, 1025 cm^{-1}, and 1057 cm^{-1}. These bands could be attributed to Q^2 stretching vibrations. In [26] Raman spectra were collected on a hydrothermally synthesized 14 Å tobermorite and the authors observed a band at 1005 cm^{-1}, interpreted as the stretching of Q^2 tetrahedra, and a weak and broad band at 850 cm^{-1}, interpreted as the occurrence of Q^1 tetrahedra. Our plombièrite sample does not show the weak and broad band related to the presence of Q^1 tetrahedra. They also observed a band at 1070 cm^{-1} [26]; according to them, it can be assigned to the stretching of CO_3 groups. However, the occurrence of CO_3 groups in plombièrite is not supported by the structural study in [4], and it can be due to superficial carbonation. According to [27], the spectral region ranging from 1040 to 1200 cm^{-1} may show band related to Si–OH bonds. Owing to the presence of silanol groups in plombièrite [28,10,4], the three bands (at 996, 1024, and 1051 cm^{-1}, respectively) could be attributed to different local environments around Q^2 tetrahedra, i.e. Si–O and Si–OH bonds. In addition to the most intense peaks, the spectrum of plombièrite shows very weak bands probably related to Ca–O vibrations and to the internal deformation of silicate tetrahedra.

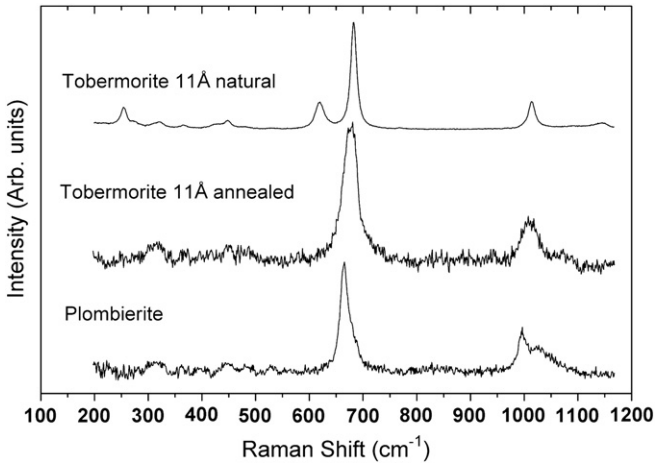

Fig. 7. Micro-Raman spectra of plombièrite from Crestmore and 11 Å tobermorite obtained through heating at 150 °C for 4 h.

Table 1
Observed frequencies (cm^{-1}) in micro-Raman spectra of plombièrite and its dehydration product, i.e. 11 Å tobermorite.

Plombièrite	11 Å tobermorite	Interpretation
310	320	Ca–O polyhedra vibrations
360		
398		Internal deformation of Si–O tetrahedra
443		(bending O–Si–O bonds)
479		
527		
664	670	Symmetrical bending Q^2
680	682	
996	1010	Symmetrical stretching Q^2
1024	1070	
1057		

The spectrum of the 11 Å tobermorite shows the same features as that observed in plombièrite, with a worse signal to noise ratio and broader bands. The most intense band is composed by two vibrations at 670 and 682 cm^{-1}, respectively, and can be interpreted as the Si–O–Si bending vibrations related to Q^2 sites. The corresponding Si–O–Si bending vibration related to Q^3 sites, which in natural 11 Å tobermorite occurs at 619 cm^{-1} [29] (Fig. 7) is definitely not present in the 11 Å dehydration product. The region of the stretching vibrations is similar to that of plombièrite, with two broad bands at 1010 and 1070 cm^{-1}, respectively. The latter can be hypothetically attributed to a superficial carbonation formed during the heating process in air.

5. Discussion

The studied specimens of natural plombièrite show thermal behaviors identical with those described by previous authors and, in particular, agree with that reported by [10] for the synthetic 14 Å tobermorite.

During dehydration, plombièrite transforms into a 11 Å tobermorite through the progressive approaching of the complex structural modules. Before its complete disappearance, the basal spacing of plombièrite diminishes down to ca. 13 Å. The newly formed 11 Å phase progressively contracts its basal spacing, reaching a value similar to that of natural 11 Å tobermorite, i.e. 11.3 Å. Notwithstanding the similarity between the basal spacings, the silicate chains of the dehydration product are single, according to the micro-Raman spectra. This conclusion agrees with that of previous authors; in addition, in [10] the possible occurrence of Q^3 site is suggested, probably as a result of stacking faults during the approaching of the complex modules. It is not clear if the 11 Å tobermorite with single chain is a metastable phase or if it could be found in geological environments. Crystals of this phase kept at room conditions maintain the same X-ray powder diffraction patterns after few years. If this kind of 11 Å tobermorite is stable, it is not possible to exclude the natural existence of specimens with single wollastonite-like chains, e.g. formed during a very mildly thermal metamorphism of plombièrite. As a matter of fact, all the natural 11 Å tobermorites for which we have structural data contain double chains.

An interesting topic is related to the nature of the 9.6 Å phase and its relationship with the 9 Å phase obtained through dehydration of normal tobermorite. In fact, whereas the former expands to a 10 Å compound upon heating, the latter is stable up to its transition into wollastonite. Finally, also the nature of this 10 Å phase and its relation with the 10 Å tobermorite described in [29] are unknown and should be investigated.

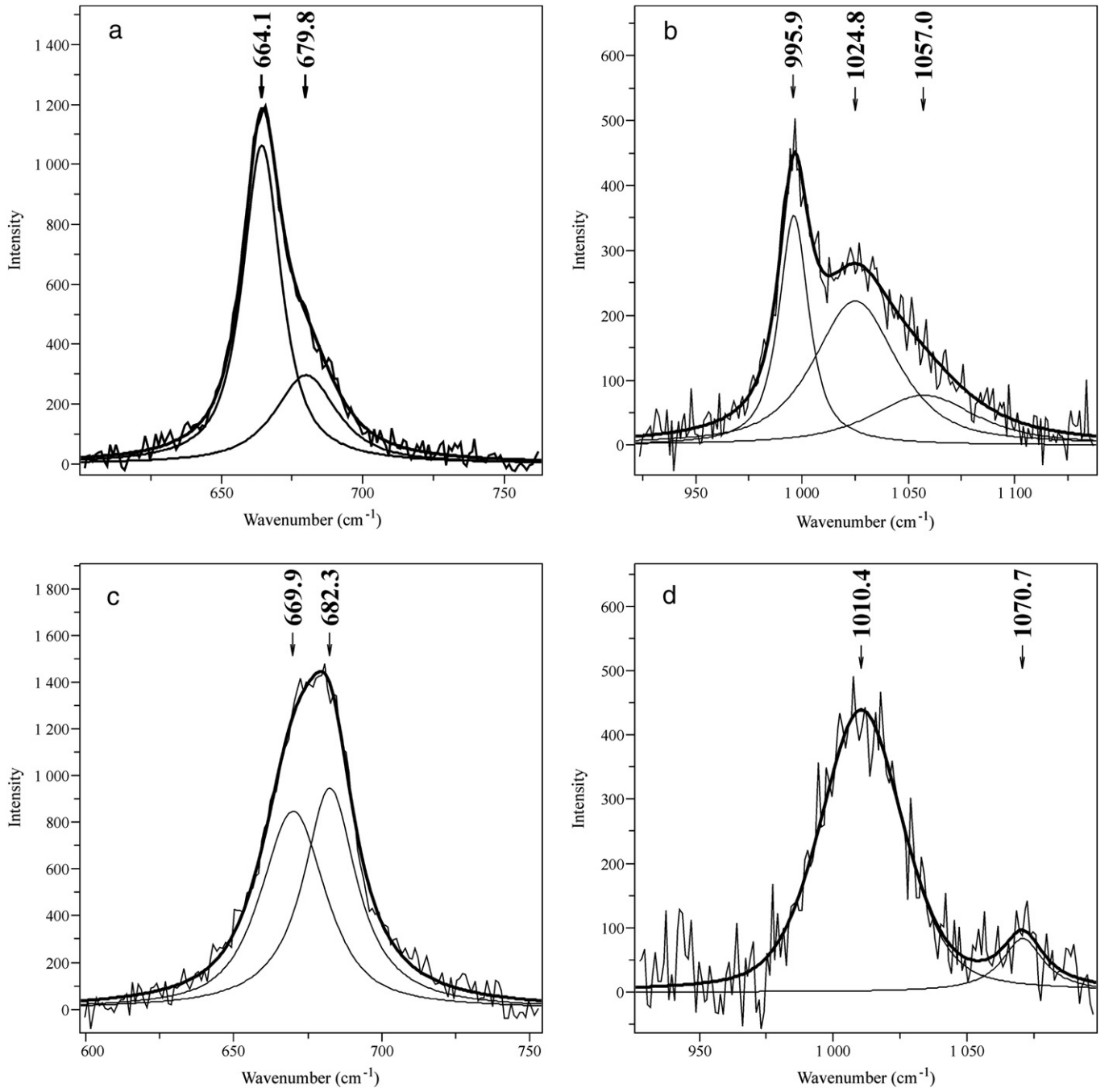

Fig. 8. The deconvolution of the micro-Raman bands of natural plombièrite (a,b) and thermally treated plombièrite (c,d). The (a) and (c) diagrams refer to the symmetrical bending, whereas the (b) and (d) diagrams refer to the symmetrical stretching of the Si – O bonds.

Acknowledgments

The constructive suggestions of the anonymous referees greatly improved the readability of the paper, and we are grateful to all them. This work was supported by the MIUR (Ministero dell'Istruzione, dell'Università e della Ricerca) through grants to the national project PRIN 2009 'Structures, microstructures and properties of minerals'.

References

[1] M. Daubrée, Mémoire sur le relation des sources thermals de Plombières avec le filons métalliféres er sur la formation contemporaine des zéolithes, Ann. Min. 13 (1858) 227–256, (in French).
[2] H.F.W. Taylor, Cement Chemistry, Thomas Telford Services Ltd., London, 1997, (450 pp.).
[3] J.D.C. McConnell, The hydrated calcium silicates riversideite, tobermorite, and plombierite, Mineral. Mag. 30 (1954) 293–305.
[4] E. Bonaccorsi, S. Merlino, A.R. Kampf, The crystal structure of tobermorite 14 Å (plombierite), a C–S–H phase, J. Am. Ceram. Soc. 88 (2005) 505–512.
[5] F. Liebau, Structural Chemistry of Silicates—Structure, Bonding, and Classification, Springer Verlag, 1985, (347 pp.).
[6] T. Mitsuda, H.F.W. Taylor, Normal and anomalous tobermorites, Mineral. Mag. 42 (1978) 229–235.
[7] V.C. Farmer, J. Jeevaratnam, K. Speakman, H.F.W. Taylor, Thermal decomposition of 14 Å tobermorite from Crestmore, Symp. Struct. Portl. Cem. Paste Concr. Spec. Rep., 90, 1966, pp. 291–299.
[8] W. Wieker, Silicationenstruktur des 14 Å-tobermorits von Crestmore und Seiner Entwässerungsprodukte, Z. Anorg. Allg. Chem. 360 (1968) 307–316, (in German).
[9] W. Wieker, A.-R. Grimmer, A. Winkler, M. Mägi, M. Tarmak, E. Lippmaa, Solid-state high-resolution ^{29}Si NMR spectroscopy of synthetic 14 Å, 11 Å and 9 Å tobermorites, Cem. Concr. Res. 12 (1982) 333–339.
[10] P. Yu, R.J. Kirkpatrick, Thermal dehydration of tobermorite and jennite, Concr. Sci. Eng. 1 (1999) 185–191.

[11] T. Maeshima, H. Noma, M. Sakiyama, T. Mitsuda, Natural 1.1 and 1.4 nm tobermorites from Fuka, Okayama Prefecture, Japan: chemical analysis, cell dimensions, ^{29}Si NMR and thermal behavior, Cem. Concr. Res. 33 (2003) 1515–1523.
[12] C. Meneghini, G. Artioli, A. Balerna, A.F. Gualtieri, P. Norby, S. Mobilio, Multipurpose imaging-plate camera for in-situ powder XRD at the GILDA beamline, J. Synchrotron Radiat. 8 (2001) 1162–1166.
[13] A.P. Hammersley, S.O. Svensson, M. Hanfland, A.N. Fitch, D. Häusermann, Two-dimensional detector software: from real detector to idealized image or two-theta scan, High Pressure Res. 14 (1996) 235–248.
[14] A.C. Larson, R.B. Von Dreele, General Structure Analysis System (GSAS), Los Alamos Nat. Lab. Rep. LAUR, 1994, pp. 86–748.
[15] B.H. Toby, EXPGUI, a graphical user interface for GSAS, J. Appl. Crystallogr. 34 (2001) 210–213.
[16] A. Le Bail, H. Duroy, J.L. Fourquet, Ab initio structure determination of $LiSbWO_6$ by X-ray powder diffraction, Mater. Res. Bull. 23 (1988) 447–452.
[17] M. Wojdyr, Fityk: a general-purpose peak fitting program, J. Appl. Crystallogr. 43 (2010) 1126–1128.
[18] C. Biagioni, I silicati idrati di calcio: assetto strutturale e comportamento termico, Ph.D. dissertation, University of Pisa, 2011, 300 pp. (in Italian).
[19] S.M. Antao, M.J. Duane, I. Hassan, DTA, TG, and XRD studies of sturmanite and ettringite, Can. Mineral. 40 (2002) 1403–1409.
[20] C. Hall, P. Barnes, A.D. Billimore, A.C. Juppe, X. Turillas, Thermal decomposition of ettringite $Ca_6[Al(OH)_6]_2(SO_4)_3\cdot 26H_2O$, J. Chem. Soc. 92 (1996) 2125–2129.
[21] Q. Zhou, F.P. Glasser, Thermal stability and decomposition mechanism of ettringite at <120 °C, Cem. Concr. Res. 31 (2001) 1333–1339.
[22] Y. Shimada, J.F. Young, Structural changes during thermal dehydration of ettringite, Adv. Cem. Res. 13 (2001) 77–81.
[23] M.R. Hartman, S.K. Brady, R. Berliner, M.S. Conradi, The evolution of structural changes in ettringite during thermal decomposition, J. Solid State Chem. 179 (2006) 1259–1272.
[24] J. Pourchez, F. Valdivieso, P. Grosseau, R. Guyonnet, B. Guilhot, Kinetic modeling of the thermal decomposition of ettringite into metaettringite, Cem. Concr. Res. 36 (2006) 2054–2060.
[25] S. Diamond, J.L. White, W.L. Dolch, Effects of isomorphous substitutions in hydrothermally-synthesized tobermorite, Am. Mineral. 51 (1966) 388–401.
[26] R.J. Kirkpatrick, J.L. Yarger, P.F. McMillan, P. Yu, X. Cong, Raman spectroscopy of C–S–H tobermorite and jennite, Adv. Cem. Bas. Mat. 5 (1997) 93–99.
[27] K. Garbev, P. Stemmermann, L. Black, C. Breen, J. Yarwood, B. Gasharova, Structural features of C–S–H (I) and its carbonation in air—a Raman spectroscopic study. Part I: fresh phases, J. Am. Ceram. Soc. 90 (2007) 900–907.
[28] X. Cong, R.J. Kirkpatrick, ^{29}Si and ^{17}O NMR instigation of the structure of some crystalline calcium silicate hydrates, Adv. Cem. Bas. Mat. 3 (1996) 133–143.
[29] C. Biagioni, E. Bonaccorsi, S. Merlino, D. Bersani, C. Forte, Thermal behaviour of tobermorite from N'Chwaning II mine (Kalahari Manganese Field, Republic of South Africa). Part II: tobermorite 10 Å—crystallographic and spectroscopic data, Eur. J. Mineral. 24 (2012) 991–1004.